

Improvement Thermomechanical Properties of Polylactic Acid via Titania Nanofillers Reinforcement

Open
Access

Mohammed Zorah¹, Izan Roshawaty Mustapa^{1,*}, Norlinda Daud¹, Nahida J.H.², N. A. S. Sudin¹, A. A. Majhool¹, Ebrahim Mahmoudi³

¹ Faculty of Science and Mathematics, University Education Sultan Idris, 35900 Tanjung Malim, Perak, Malaysia

² Applied Science Department, University of Technology, Baghdad, Iraq

³ Faculty of Engineering and Built Environment, University Kebangsaan Malaysia, Malaysia

ARTICLE INFO

Article history:

Received 27 February 2020

Received in revised form 30 March 2020

Accepted 2 April 2020

Available online 24 April 2020

ABSTRACT

Poly lactic acid (PLA) is a useful alternative to petrochemical commodity material used in food packaging, due to its low thermal stability and poor crystallization behaviour, it needs to improve its properties in namely terms of thermal and mechanical performance. Neat PLA was reinforced nanofiller TiO₂ (titania) to improve its characteristics. Thus, the film of neat PLA and PLA nanocomposites were prepared using solvent casting and hot press methods. Diverse techniques characterized As-prepared films. To enhance the PLA miscibility, TiO₂ nanoparticles were homogeneously dispersed in the PLA matrix to attain a low degree of agglomeration as explained by Field Emission Scanning Electron Microscopy (FESEM). Both XRD and differential scanning calorimetry (DSC) analyses of the reinforced nanocomposites disclosed an improvement in their crystallinity increased from 17.52 to 30.91. The dynamic mechanical analysis (DMA) indicated that the storage modulus was improved with increased TiO₂ content, increased from 3.13 GPa to 3.26 GPa. Thermogravimetric analysis (TGA) results show that the addition of nanofiller improved thermal stability of the PLA nanocomposites was modified. On the other hand, the reinforced PLA nanocomposites with improved biodegradable behavior were shown to be the potential substitute of conventional petrochemical-based polymers widespread in the food packaging industries.

Keywords:

PLA nanocomposites; TiO₂ nanoparticle; reinforcement; food packaging

Copyright © 2020 PENERBIT AKADEMIA BARU - All rights reserved

1. Introduction

Traditionally, the plastics produced from petroleum derivatives have been applied extensively in the different packaging industry because of their low price, softness, lightness, wide accessibility and their favorable features such as transparency, brightness, and plasticity. However, these plastics

* Corresponding author.

E-mail address: izan.mustapa@gmail.com (Izan Roshawaty Mustapa)

derived from fossil fuel resources due to their very low biodegradability remained the major environmental concern [1,2].

The release gases from the thermal degradation of these plastics cause the greenhouse effect and global warming. Furthermore, this low biodegradability related waste accumulation can cause great damage to living organisms, severe ecological imbalance, and health hazards. Due to the unsuccessful recycling of mixed plastics including waste burial and burning large quantities of waste plastics [3-5]. With the escalating consumer's demand for resilient products, research issues related to the development of biocompatible materials with functional properties became worth examining. It has been realized that using edible, active, and biodegradable films, the quality of the qualities and nutritional values of the food products can be improved [6-8].

Through the microorganisms, enzymatic action biodegradable polymers are decomposed into simple molecules such as carbon dioxide (CO_2), methane (CH_3), water (H_2O), several inorganic compounds, and biomass [9]. Currently, some biodegradable materials obtained from green resources such as polylactic acid (PLA) are categorized as bioplastics [10]. Besides biocompatibility and biodegradability attributes PLA has interesting physical properties. This linear aliphatic thermoplastic polyester is derived entirely (100%) from renewable resources such as sugar, corn, potatoes, and beet. The most common route for industrial production of high molecular weight PLA is the ring-opening polymerization (ROP) of the lactide monomer formed from lactic acid. It is produced by the fermentation of renewable agricultural resources [10-12]. Industrial PLA is mostly polymerized from L-lactide and D, L-lactide, where the L-isomer is the main fraction. PLA is an emergent candidate for consumer products such as packaging due to its transparency, degradability, low toxicity, and environmentally benign characteristics. In addition, PLA has better thermal processability than other biopolymers and requires between 20-25% less production energy than polymers derived from petroleum. Nevertheless, some shortcomings, including high brittleness, poor crystallization, and weak barrier characteristics of PLA that limit its current users need to be overcome [13-15].

In recent times, nanocomposites materials became promising due to their customized properties where emergent properties are focused on sundry applications. To improve the dynamic properties of PLA, inorganic nanoparticles were added and nanocomposites were achieved. The development of various new properties in the blended product from individual components were attributed to the specific interactions between the nanoparticles and the polymer matrix [12,16]. Therefore, the nanoparticles inclusion in PLA is regarded as an effective strategy to modify its properties and control the degradation behaviour in different media [17]. Several interesting properties of TiO_2 such as strong antibacterial activity against diverse microorganisms (including algae, viruses, fungi, and bacteria), photocatalytic activity, high stability, good mechanical properties, non-flammable, resistance to corrosion, intense UV absorption, low cost, and nontoxicity make it beneficial for many applications [1,18-20].

TiO_2 nanoparticles are included into the bio-plastics because of dual reasons: (i) the absorption of most of the UV radiation, thereby preventing the polymer degradation from environmental aging of the plastics due to UV light exposure; (ii) presence of titania nanoparticles can inhibit the bacterial growth to certain extent; (iii) resistant to thermal degradation and may prevent the formation of harmful biofilms [21]. Due to these notable attributes, TiO_2 nanoparticles have been used extensively for diverse purposes. TiO_2 exists in three crystalline polymorphs, including namely rutile, anatase, and brookite. Rutile is the most stable phase, whereas anatase and brookite are the metastable phases at all temperatures. Both these phases can transform into rutile one upon heating, and the anatase phase is the chemically most reactive [22]. Besides, embedment of nanofillers into new

generation food packaging materials can improve some of their key properties such as flexibility and strength, the barrier to gases, thermal stability, and higher resistance to heat and cold [23].

In this present study, considering the promising bio-plasticity of PLA towards food-packaging, we determined the improved thermomechanical properties of TiO₂ nanofillers reinforced PLA synthesized by unified solvent casting and hot press method. Detail data analyses of as-prepared TiO₂ nanofillers embedded PLA matrix revealed significant improvements in its storage modulus and thermal stability. It was argued that the nanoscale dispersion of TiO₂ could produce a large surface area and high aspect ratio, wherein the reinforcement efficiency of the composites was significantly enhanced.

2. Experimental

2.1 Materials

High purity analytical grade PLA 2002D was obtained in pellet form from Natureworks Co., Minnetonka, USA. TiO₂ nanoparticles with a mean particle size below 100 nm (purity 99.5%) were purchased from Sigma Aldrich (USA).

2.2 Preparation of PLA/TiO₂ Nanocomposites

To prepare the PLA–TiO₂ nanocomposites film, first, the PLA pellets were oven-dried by heating at 60 °C for a day to eliminate the moisture contents. The amount of PLA was estimated using the requisite ratio of PLA to TiO₂. Next, PLA was dissolved in a beaker that contained the THF solvent of volume 50 mL. The solution was constantly stirred before being placed in a magnetic hotplate at 60 °C for 6 h. Later, the desired nanofillers (TiO₂ of 0.5% w/w) were included in the PLA solution and stirred continuously for 1 h. The mechanical stirrer and ultrasonicator were used to disperse the TiO₂ in the mixture for about 1 h and 30 min. After that, the mixture was casted onto a Petri dish and then kept back for a day at room temperature for complete evaporation of the solvent forming a thin film of modified PLA with nanofillers of different thicknesses. The sample was dried in an oven (60 °C) for a day to ensure complete solvent removal. The same procedures were followed to prepare other modified PLA films with different content of TiO₂ (2.0, 3.5, 5.0, and 7.5% w/w). Finally, the obtained samples were pressed in a hot compression machine to divide them in equal size and thickness by avoiding the formation of the bubbles. Table 1 summarizes the details of PLA–TiO₂ nanocomposites.

Table 1
Identification of abbreviations for PLA-TiO₂ nanocomposites

Composites	PLA (wt.%)	Nanoparticle (wt.%)
PLA	100	0
PLATi0.5	99.5	0.5
PLATi2.0	98.0	2.0
PLATi3.5	96.5	3.5
PLATi5.0	95.0	5.0
PLATi7.5	92.5	7.5

2.3 Characterizations of PLA/TiO₂ Nanocomposites

The surface morphologies of the prepared nanocomposites were analyzed by FESEM (Hitachi SU8020 and JEOL JSM-7600F and a 15 kV (QUANTA FEG 450). The system was set at a high vacuum condition with two different accelerating voltages, each of 5 kV. Before the morphology analyses.

Dynamic mechanical analysis (DMA) was conducted on a TA instrument (DMA Q 800). The sample of dimension (30 mm × 8 mm × 0.5 mm) was heated from 25 to 160 °C at the scanning rate of 2 °C per min with regulated sinusoidal strain. The DMA measurement was to provide storage modulus (E'), loss modulus (E''), and damping factor ($\tan \delta$) data. Differential scanning calorimetric (DSC) tests were performed using a TA Instruments (DSC Q20 series). In every test, about 4 to 7 mg of each PLA/TiO₂ nanocomposites was encapsulated in an aluminum pan, and an empty sample pan served as a reference. First, the thermal history of the sample was removed by heating it from 30 °C to 180 °C at scanning a rate of 10 °C/min. Then, the sample was held at 180 °C for 10 min followed by cooling at 30 °C at scanning a rate of 2 °C/min. Next, the thermal performance of the sample was recorded by reheating it from 30 °C to 180 °C at scanning a rate of 2 °C/min. The glass transition temperature (T_g), cold crystallization temperature (T_{cc}), melting temperature (T_m) and melting enthalpy (ΔH_m) were determined from the second heating scan. The degree of crystallinity (X_c) was calculated using Eq. (1) [24].

$$X_c = \frac{\Delta H_m - \Delta H_{cc}}{\Delta H_m^*} \times 100 \quad (1)$$

where ΔH_{cc} (in J/g) and ΔH_m (in J/g) are the respective enthalpies of the crystallization and the fusion of the PLA nanocomposites, ΔH_m^* (93.1 J/g) is the heat of fusion of 100% PLA [24].

Thermogravimetric analysis (TGA) of the as-prepared nanocomposites was carried out using a TA instruments (Q-500). About 5 to 10 mg of each composite was separately placed onto the sample holder containing a clean platinum pan. Next, it was carried to the beam balance and the oven was closed before being heated at the rate of 10 °C/min from room temperature to 600 °C in the nitrogen atmosphere.

3. Results and Discussion

3.1 Cross Section Morphology of PLA Nanocomposites

The FESEM cross - section morphology of the PLA nanocomposites (Figure 1) was carried out to evaluate the dispersion and distribution of TiO₂ nanoparticles inside the biodegradable polymer matrix. Furthermore, qualitative analyses on phase dispersion, polycrystalline morphologies, and interfacial strength were performed. The images of nanocomposites were taken in areas where the films were earlier in cryogenically fractured surfaces under liquid nitrogen. The morphology of the neat PLA film was observed to be flat without any trace of matrix tearing, the formation of holes and cavities, wherein TiO₂ nanoparticle was entirely embedded into the PLA matrix. Moreover, the incorporated TiO₂ nanoparticle was dispersed well and distributed quite uniformly and homogeneously inside the PLA matrix without any considerable agglomeration for TiO₂ content up to 3.5 wt%. This indicated excellent dispersion of TiO₂ nanoparticle at its lower wt%. Moreover, at higher contents up to 5 wt% and above these nanofillers revealed an enhanced agglomeration tendency.

This agglomeration trend of the nanocomposites at higher TiO₂ contents was majorly ascribed to the absence of any surface treatment on the used TiO₂, where interaction among Ti and OH groups on the surface became significant.

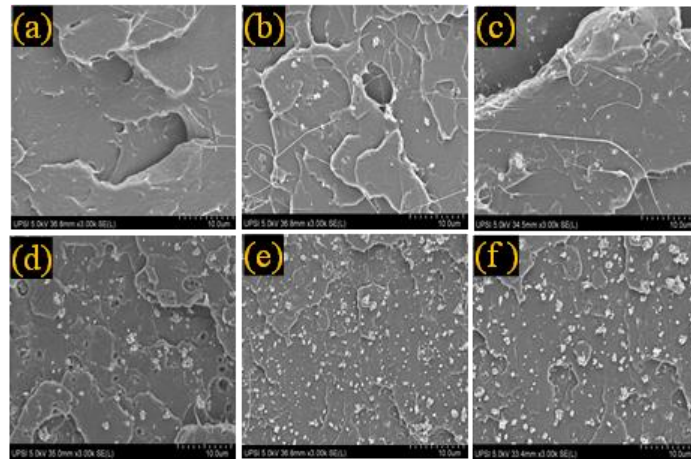


Fig. 1. FESEM images at 5000 \times magnifications for (a) neat PLA, (b) PLATi0.5, (c) PLATi2.0 and (d) PLATi3.5, (e) PLATi5.0, (f) PLATi7.5

Additionally, the influence of van der Waals forces played a major role in the synthesis of TiO₂/PLA nanocomposites via solvent casting solution through direct dispersion of TiO₂ into the PLA matrix. Such dispersion of TiO₂ into the PLA matrix could have a direct effect on the physical traits of the nanocomposites, wherein the role of TiO₂ at the individual level becomes significant.

3.2 XRD Scattering Angle of PLA Nanocomposites

Figure 2 illustrates the XRD pattern of prepared PLA and PLA/TiO₂ nanocomposites which clearly showed the influence of TiO₂ incorporation into the PLA matrix in terms of various crystalline peaks. The characteristic crystalline peaks of PLA and PLA/TiO₂ nanocomposites were observed, wherein neat PLA and all nanocomposites revealed a broad peak around $2\theta = 16.5^\circ$ allocated to the semi-crystalline structure. The occurrence of crystalline peaks in the prepared nanocomposites were allotted to the diffraction from (110) and (200) lattice planes of the α -crystalline phase of PLA [25]. Furthermore, neat PLA films did not show any sharp crystalline peak. With the increase of TiO₂ contents as filler in the PLA polymer matrix, the crystalline peaks belonging to the TiO₂ became more prominent. The appearance of these sharp diffraction peaks centered at 2θ value of 27.5° , 36° , 41.2° , and 54.3° , were assigned to the rutile phase of TiO₂ which was consistent with other reported values [26,27].

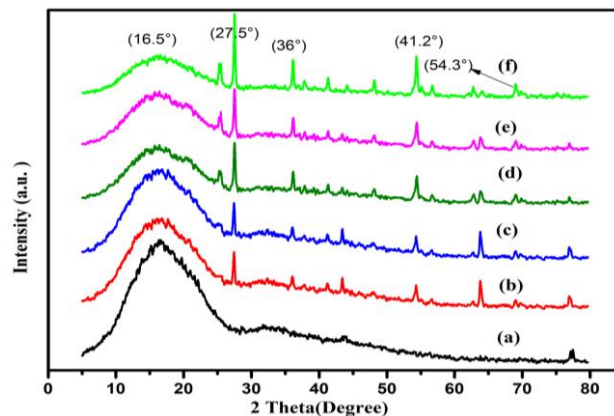


Fig. 2. XRD pattern (a) neat PLA, (b) PLATi0.5, (c) PLATi2.0, (d) PLATi3.5, (e) PLATi5.0, and (f) PLATi7.5

3.3 Dynamic Mechanical Properties of Nanocomposites

Storage modulus or elastic modulus (E') is a measure of the stiffness of the materials. Figure 3 shows the variation of E' as a function of temperature for the nanocomposites with and without TiO_2 embedment. This provides a clear view of the molecular mobilities alteration in PLA/ TiO_2 nanocomposites compared to neat PLA. The value of E' provided the information related to the storage of maximum energy in the nanocomposites during one oscillation cycle. It also described the mechanical stiffness and the load-bearing ability of the nanocomposites as a function of temperature and frequency. Usually, the E' and Young modulus are related to each other through materials' stiffness [28].

In the low temperatures domain (30 to 50 °C) the nanocomposites revealed the glassy phase with brittle and rigid characters. In the mid temperature's region (59.63° C to 61.22°C) all the nanocomposites disclosed a usual semi-crystalline polymeric nature with an outsized reduction in the E' value, which corresponded to the glass transition temperature (T_g) region, wherein the peaks in the loss modulus and damping factor appeared. Furthermore, these nanocomposites changed their behavior from brittle and rigid to soft and ductile types. The high-temperature region (above 60 °C) corresponded to the rubbery state where the stiffness was very low, and the nanocomposites could retain its softness and elastic character.

The increase in the E' values for the nanocomposites with the increase in TiO_2 (nanofiller embedment) loading was consistent with other findings [4,29]. However, it was argued that the nanofillers content should be below a certain limit so that the value of E' must not drop notably. The observed reduction in the E' values can be ascribed to the agglomeration tendency of TiO_2 and imperfect dispersion, which led to the ineffective transfer of stress at the interfacial regions of the PLA matrix and inter-phases. The FESEM morphologies (Figure 1) of the nanocomposites supported this observation. The agglomerated TiO_2 were connected to each other and arrested the molecular movement at the point of contact inside the inter-phases, thus enhancing the moduli and stiffness of the resultant nanocomposites.

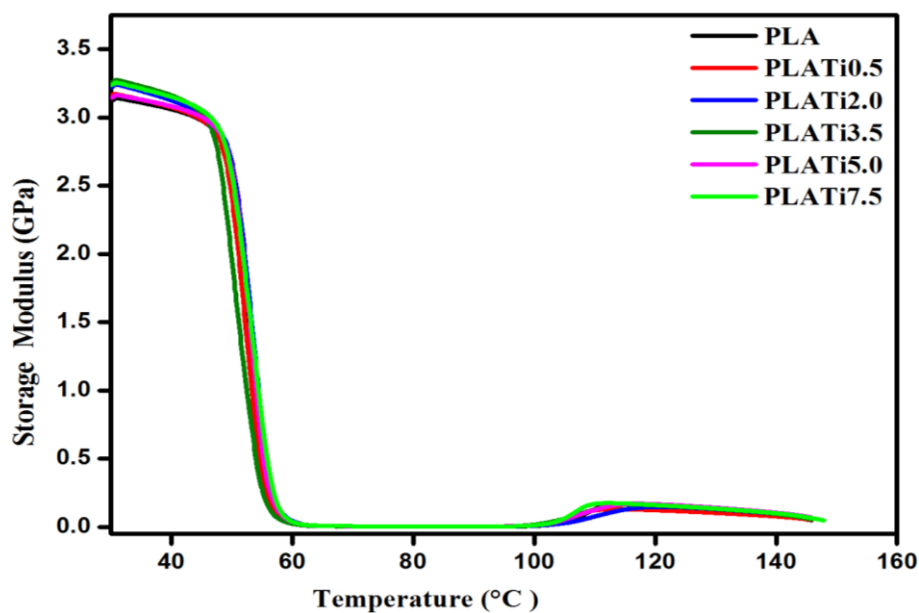


Fig. 3. Temperature-Dependent Variation in the Storage Modulus of neat PLA Various PLA Nanocomposites

The PLA/TiO₂ nanocomposites also showed a decrease in the E' values with an increase in temperature. In the lower temperature region, the polymer chains were fairly stiff however, with increasing temperature, they became more flexible. The movement of polymer chains was rapid because of the higher mobility of the segments, thus leading to lesser stiffness and a decrease in the E' values as expected. Nevertheless, the observed increasing trend in the E' around 100 °C was attributed to the onset of cold crystallization of PLA and subsequent growth of tiny spheroidal mass of crystals (spherulites) in the nanocomposites [30].

The values of loss modulus (E'') measure the materials' viscosity in terms of the energy loss in the form of heat in the presence of stress or deformation cycle. Figure 4 illustrates the variation of E'' as a function of temperature for the nanocomposite's films without and with TiO₂ embedment. A higher value of E'' signifies higher viscosity, marking higher damping characteristics. Both below and above T_g (maximum of E''), the E'' value for pristine PLA film was more compared to TiO₂ embedded PLA film. These lower peak values of E'' for the prepared nanocomposites were ascribed to the TiO₂ incorporation facilitated an increase in the number of chain segments within the free volume of the PLA matrix. The inclusion of TiO₂ could have hindered the relaxation process of polymeric chains within complex networks. Furthermore, the addition of TiO₂ as nanofiller led to a reduction in the nanocomposite's viscosity compared to neat PLA matrix. Conversely, the E' values started increasing at around 100 °C because of the cold crystallization process of PLA and the formation of spherulites in the synthesized bio composites [30,31].

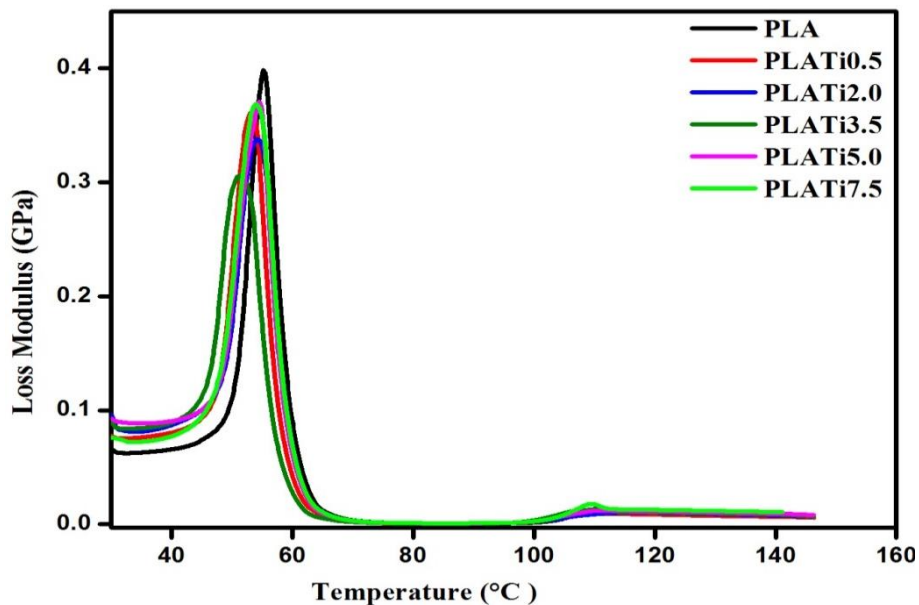


Fig. 4. Temperature -Dependent Variation in the Loss Modulus of neat PLA Various PLA Nanocomposites

Figure 5 shows the temperature dependent variation in the damping factor ($\tan \delta$) of various PLA/TiO₂ nanocomposites with and without TiO₂ incorporation. Irrespective of the TiO₂ contents, the peak values of $\tan \delta$ for the PLA/TiO₂ nanocomposites were reduced compared to neat PLA. This lowering in the $\tan \delta$ values for the nanocomposites because of TiO₂ (nanofillers) embedment is useful for thermo-mechanical applications.

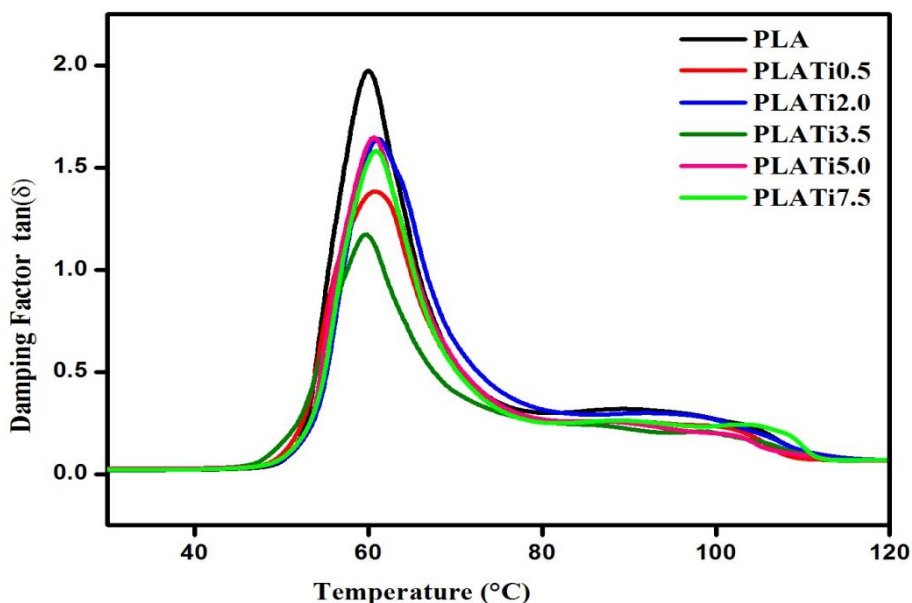


Fig. 5. Temperature -Dependent Variation in the Damping Factor of neat PLA Various PLA Nanocomposites

The value of $\tan \delta$ for all nanocomposites first reached a maximum around T_g and then decreased rapidly, indicating the softening tendency of the PLA/TiO₂ nanocomposites. The values of both $\tan \delta$ and T_g were greatly sensitive to the entrenchment of nanofillers volume fraction in the polymeric matrix. Table 2 enlists the measured dynamic mechanical attributes of various PLA/TiO₂ nanocomposites with and without TiO₂ embedment. Clearly, neat PLA film showed the maximum value of $\tan \delta$ (1.97), implying the highest molecular movement.

Table 2

Dynamic mechanical characteristics of various PLA nanocomposites with and without TiO₂

Samples	E' (GPa)	E'' (GPa)	T _g (°C)	tan δ
PLA	3.13	0.080	59.9	1.97
PLATi0.5	3.21	0.081	60.69	1.38
PLATi2.0	3.23	0.115	61.22	1.61
PLATi3.5	3.26	0.092	59.63	1.20
PLATi5.0	3.20	0.077	60.65	1.64
PLATi7.5	3.24	0.074	60.82	1.58

3.4 Thermal Behavior of PLA Nanocomposites

It is established that nanoparticles substantially influence the growth and nucleation processes of materials. In the present case, the incorporated TiO₂ nanoparticles so-called nanofillers acted as nucleating agents in the PLA polymer, thereby produced improved properties. PLA is a semi-crystalline polymer, its mechanical properties could depend significantly on the degree of crystallization. Consequently, the effect of polymer crystallization on the improvement of the mechanical properties of PLA/TiO₂ nanocomposites was evaluated. Figure 6 displays the DSC curves of nanocomposites containing various amounts of TiO₂ compared to neat PLA (without TiO₂). It also shows the important parameters: glass transition temperature (T_g), melting temperature (T_m) and crystallization temperature (T_c). The first and second DSC heating cycle was performed with the scanning rate of 10 °C/min and 2 °C/min respectively.

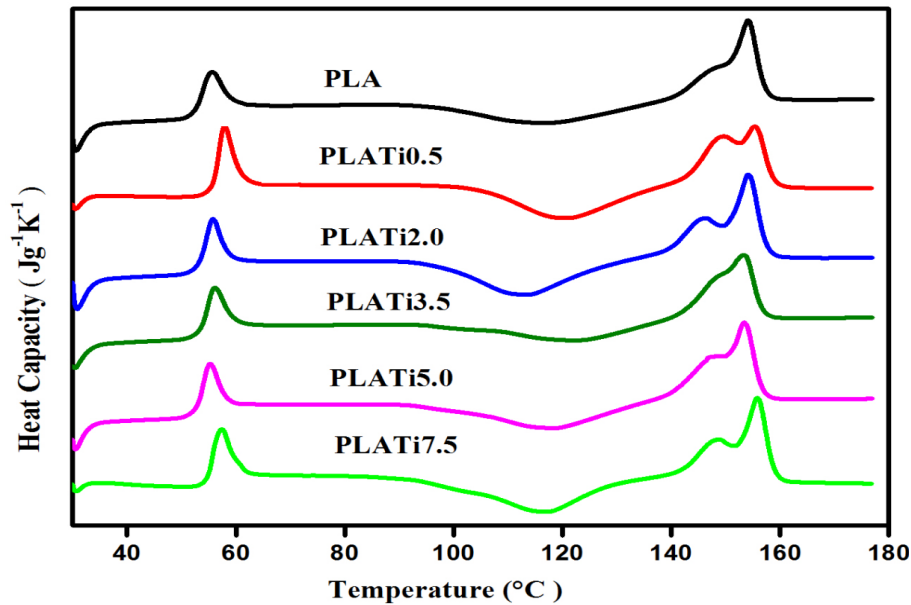


Fig. 6. DSC Curves of PLA Nanocomposites Compared to Neat PLA in the First Cycle of Heating

Neat PLA revealed a T_g and T_m value of 53 °C and 153.0 °C, respectively, as reported earlier [32]. Furthermore, the location of T_g , T_{cc} , and T_m were shifted with the change in TiO_2 contents (0.5, 2, 3.5, 5, and 7.5 wt%). Figure 7 shows the DSC curves of all the prepared nanocomposites compared to neat PLA. The crystallization processes of nanocomposites became prominent during heating (cold crystallization), and a peak was developed. The value of T_m of the nanocomposites was close to 154 °C, wherein various transition temperatures were not significantly affected due to the embedment of TiO_2 in the PLA matrix.

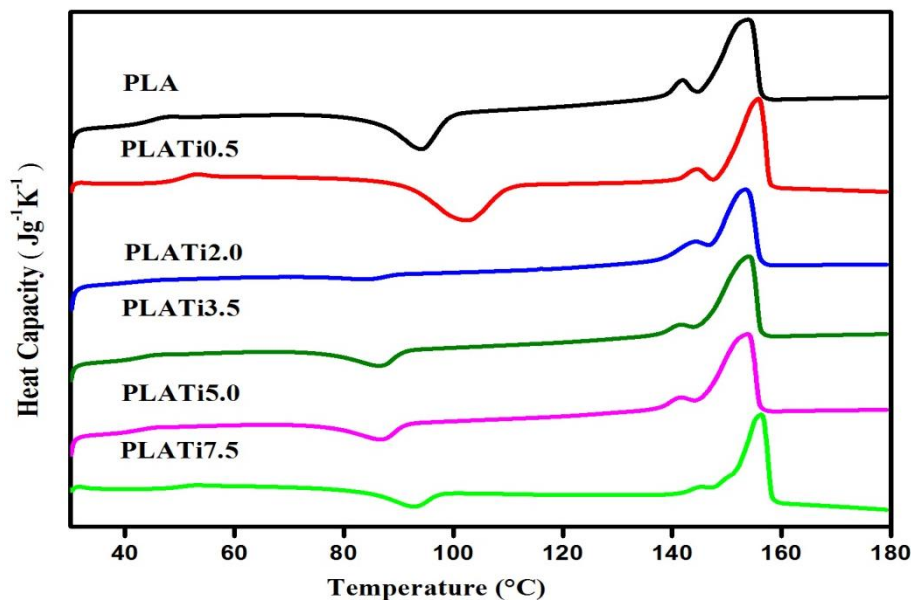


Fig. 7. DSC Curves of all the PLA Nanocomposites Compared to Neat PLA in the Second Cycle of Heating

Neat PLA and TiO_2 embedded PLA both disclosed two melting peaks with the dominant one at the higher temperature. These results are in good agreement with other reported data in the literature on PLA and its nanocomposites [31,32]. Usually, neat PLA shows two melting peaks. At a

low rate of scanning, tiny and irregular crystallites have enough time for the melting and recrystallization process, which can majorly be explained by melt-recrystallization model [30].

Table 3 summarizes the thermal parameters of various PLA/TiO₂ nanocomposites with and without TiO₂ (nanofillers) embedment. The crystallinity percentage in the nanocomposites can be obtained from the DSC data analyses (Eq. (1)). The enthalpy of fusion for crystalline PLA (100% crystallinity) was found to be 93.1 J/g. Furthermore, the crystallinity degree of nanocomposites was improved with an increase in the TiO₂ contents. This TiO₂ concentration dependent enhanced crystallinity amount in the nanocomposites was ascribed to the accelerated nucleation effects. The PLA nanocomposites containing 2.0 and 3.5 wt-% of TiO₂ revealed the optimum crystallinity; however, the crystallinity of the composites decreased at high content of TiO₂. The occurrence of reduced crystallinity with the increase of TiO₂ content beyond 3.5 wt-% was attributed to the aggregation of TiO₂, where highly uniform dispersion of TiO₂ could form stronger interaction among them in the PLA matrix, thereby inducing accelerated nucleation and growth. The observed discrepancy in the T_g values obtained from DSC and DMA is primarily due to the use of different sollicitation modes, which are not comparable. The value of T_g obtained from DMA was shifted toward higher temperatures than those attained by DSC analyses which were ascribed to the frequency dependent factor.

Table 3

Thermal parameters of various PLA nanocomposites with and without TiO₂

Samples	T _g (°C)	T _c (°C)	T _{cc} (°C)	ΔH _{cc} (J/g)	T _{m1} (°C)	T _{m2} (°C)	ΔH _m (J/g)	χ _c (%)
PLA	53.00	92.10	94.20	18.80	141.90	153.00	37.72	17.52
PLATi0.5	54.00	92.35	95.50	12.30	140.00	153.20	30.10	21.22
PLATi2.0	55.69	95.50	93.10	1.27	142.80	153.70	32.30	30.91
PLATi3.5	55.15	95.00	93.20	7.39	140.70	154.10	34.90	29.52
PLATi5.0	56.00	92.50	93.60	8.40	140.80	153.95	34.50	25.47
PLATi7.5	55.90	92.00	94.00	9.00	141.00	153.70	34.10	26.23

3.5 Thermal Stability of PLA Nanocomposites

Figure 8 and Figure 9 present the TGA and DTG curves of various PLA/TiO₂ nanocomposites with and without TiO₂ (nanofillers) embedment. The thermal degradation of the different samples was evaluated in one step, apart from a slight weight loss below 100 °C, which can be attributed to the evaporation of adsorbed water. The appearance of the plateau starting from 285 °C was due to the decomposition of nanocomposites. After that, a significant mass loss is observed, which corresponds to the decomposition of the PLA. Two indicators, such as the onset degradation temperature (T_{onset}) and destabilization temperature at weight loss of 50% (T_{50%}) were used to characterize the onset and the structural decomposition of the nanocomposites.

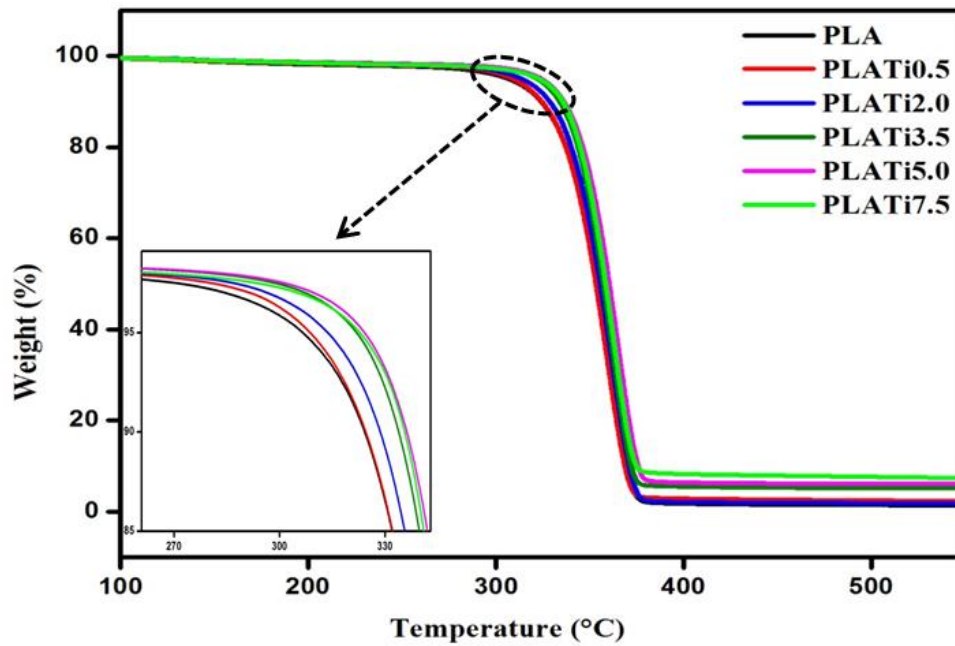


Fig. 8. TGA Curves of Various PLA Nanocomposites with and Without TiO₂

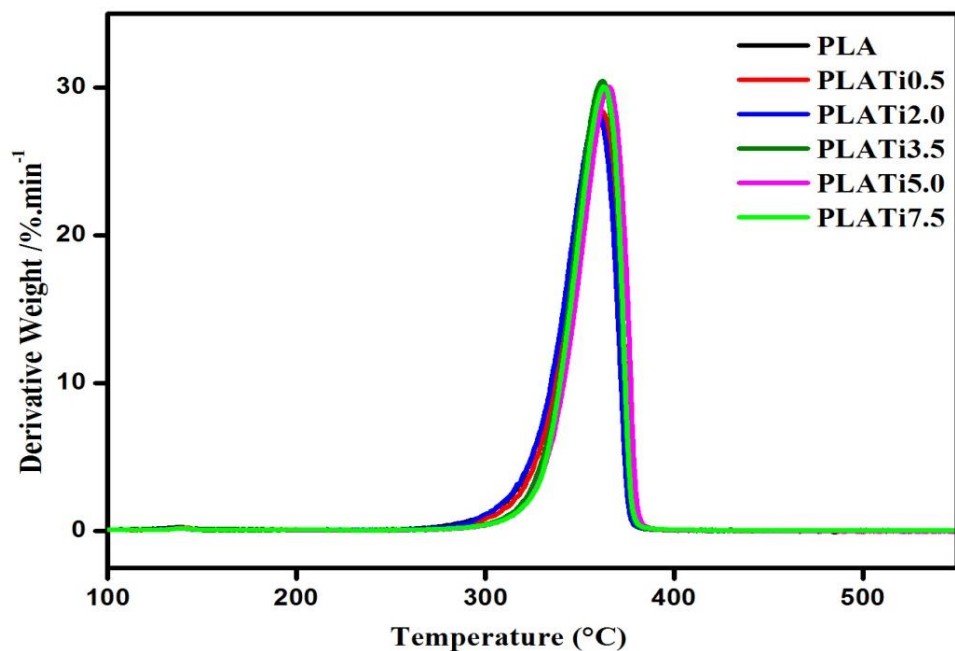


Fig. 9. DTG Curves of Various PLA Nanocomposites with and Without TiO₂

Table 4 enlists the (T_{end}) referred to end decomposition and the values of maximum derivative weight (T_{max}) obtained from a derivative mass loss curve and the mass residue of the samples (char residue) at 525 °C. The weight loss of $T_{5\%}$ was defined as the initial decomposition temperature. Primarily, TiO₂ might have acted as a barrier of heat in the early phases of thermal decomposition and reduced the molecular movements of PLA molecules adjacent to the TiO₂.

Table 4
Thermal properties of various PLA/TiO₂ nanocomposites with and without TiO₂

Composites	T _{onset} (°C)	T _{50%} (°C)	T _{end} (°C)	T _{max} (°C)	Char Residue (%)
PLA	288.7	353.8	378.5	360.2	1.44
PLATi0.5	291.1	353.4	376.0	360.5	1.87
PLATi2.0	291.3	355.0	376.4	361.1	2.80
PLATi3.5	307.4	357.2	377.1	362.2	5.21
PLATi5.0	310.0	360.0	379.0	366.5	6.30
PLATi7.5	305.2	358.1	378.1	364.3	8.62

It is obvious to note that the onset degradation temperature of nanocomposites shifts to a higher temperature with the increase for neat PLA, the value of T_{onset} was about 288.7 °C and the complete degradation occurred around 378.5 °C, which was lower compared to PLA/TiO₂ nanocomposites (Figure 9). Both T_{onset} and T_{end} for the nanocomposites were shifted to a higher value compared with the neat PLA where the residue of the neat PLA film (1.44%) was lower. The residue for these nanocomposites was ranged from 1.87% to 8.62% when TiO₂ contents in the PLA matrix were varied from 0.5 wt% to 7.5 wt%, respectively. This indicated constant mass retention of the nanocomposites at the end of each TGA scan (Table 4) wherein the observed values were close to the theoretical estimates. TGA being an analytical technique is highly sensitive to the actual contents of TiO₂; thus, the differences were consistent with the amount of TiO₂ added into the PLA matrix. This observation suggested an excellent dispersion of TiO₂ within the PLA matrix and tallied well with other reports [31,33]. The thermal stability of the nanocomposites was improved. This modification in the thermal stability of nanocomposites due to TiO₂ embedment can be ascribed to varieties of chemical and physical processes.

4. Conclusions

This work attempted to improve some drawbacks related to the thermomechanical properties of biodegradable PLA biopolymer. To achieve this, nanofiller TiO₂ was incorporated into PLA and PLA/TiO₂ nanocomposites were synthesized using solvent casting united hot press methods. These TiO₂ nanoparticles reinforced PLA revealed improved biodegradable qualities. The homogeneous dispersion of TiO₂ in the polymer matrix could produce a very low degree of agglomeration, thus enhanced biodegradable attributes. The mechanical, morphological structural, and thermal characterizations of the as-prepared nanocomposites were made. FESEM analyses disclosed good incorporation of nanofillers with homogeneous surface morphology. The XRD analyses of nanocomposites showed crystallization without any inhibition. The DMA of nanocomposites displayed enhancement in the thermo-mechanical properties, wherein the addition of TiO₂ caused an increase in the storage modulus (stiffness) and a decrease in the (tan δ) values. The DSC measurement verified insignificant effects of TiO₂ on the T_m, but had a prominent effect on the T_{cc} and X_c. The TGA analysis of nanocomposites exhibited an increase in the final residue with the increase in TiO₂ content, confirming its excellent dispersion. The observed enhancement in the thermal stability, the modulus, and elastic limit of the PLA was ascribed to the TiO₂ reinforcement mediated effects. It was concluded that materials with low fill percentage can be effective to get excellent distribution and orientation of the particles in the polymeric matrix. It was established that the nanocomposites with excellent biodegradability and thermo-mechanical traits are potential for industrial applications, especially in food packaging.

References

- [1] Mohr, L. C., A. P. Capelezzo, C. R. D. M. Baretta, M. A. P. M. Martins, M. A. Fiori, and J. M. M. Mello. "Titanium dioxide nanoparticles applied as ultraviolet radiation blocker in the polylactic acid biodegradable polymer." *Polymer Testing* 77, no. 8 (2019): 1-10.
<https://doi.org/10.1016/j.polymertesting.2019.04.014>
- [2] Burgos, Nuria, Daniel Tolaguera, Stefano Fiori, and Alfonso Jiménez. "Synthesis and characterization of lactic acid oligomers: Evaluation of performance as poly (lactic acid) plasticizers." *Journal of Polymers and the Environment* 22, no. 2 (2014): 227-235.
<https://doi.org/10.1007/s10924-013-0628-5>
- [3] Haider, Tobias P., Carolin Völker, Johanna Kramm, Katharina Landfester, and Frederik R. Wurm. "Plastics of the future? The impact of biodegradable polymers on the environment and on society." *Angewandte Chemie International Edition* 58, no. 1 (2019): 50-62.
<https://doi.org/10.1002/anie.201805766>
- [4] Huang, Ying, Tongwen Wang, Xiaolei Zhao, Xinlong Wang, Lu Zhou, Yuanyuan Yang, Fenghui Liao, and Yaqing Ju. "Poly (lactic acid)/graphene oxide-ZnO nanocomposite films with good mechanical, dynamic mechanical, anti-UV and antibacterial properties." *Journal of Chemical Technology & Biotechnology* 90, no. 9 (2015): 1677-1684.
<https://doi.org/10.1002/jctb.4476>
- [5] Kamdem, Donatien Pascal, Zhu Shen, Omid Nabinejad, and Zuju Shu. "Development of biodegradable composite chitosan-based films incorporated with xylan and carvacrol for food packaging application." *Food Packaging and Shelf Life* 21, no. 9 (2019): 100344.
<https://doi.org/10.1016/j.fpsl.2019.100344>
- [6] Kanmani, Paulraj, and Jong-Whan Rhim. "Physical, mechanical and antimicrobial properties of gelatin based active nanocomposite films containing AgNPs and nanoclay." *Food Hydrocolloids* 35, no. 3 (2014): 644-652.
<https://doi.org/10.1016/j.foodhyd.2013.08.011>
- [7] Seligra, Paula González, Carolina Medina Jaramillo, Lucía Famá, and Silvia Goyanes. "Biodegradable and non-retrogradable eco-films based on starch-glycerol with citric acid as crosslinking agent." *Carbohydrate Polymers* 138, no. 3 (2016): 66-74.
<https://doi.org/10.1016/j.carbpol.2015.11.041>
- [8] Shojaeiarani, Jamileh, Dilpreet Bajwa, Long Jiang, Joshua Liaw, and Kerry Hartman. "Insight on the influence of nano zinc oxide on the thermal, dynamic mechanical, and flow characteristics of Poly (lactic acid)-zinc oxide composites." *Polymer Engineering & Science* 59, no. 6 (2019): 1242-1249.
<https://doi.org/10.1002/pen.25107>
- [9] del Rosario Salazar-Sánchez, Margarita, Sergio David Campo-Erazo, Héctor Samuel Villada-Castillo, and José Fernando Solanilla-Duque. "Structural changes of cassava starch and polylactic acid films submitted to biodegradation process." *International Journal of Biological Macromolecules* 129, no. 3 (2019): 442-447.
<https://doi.org/10.1016/j.ijbiomac.2019.01.187>
- [10] Osmani, Sharifah Nur Aqilah Wan, Fathilah Ali, and Sarah Amalina Adli. "Effect of acid hydrolysis treated pineapple fiber in plasticized polylactic acid composite." *Significance* 50, no. 1 (2018): 14-18.
- [11] Jimat, Dzun N., Faridah Ariffin, Maimunah Asem, and Sarina Sulaiman. "Characterization of biodegradable composite based on polycaprolactone/starch reinforced with sugarcane bagasse microfibrillated cellulose." *Journal of Advanced Research in Materials Science* 39, no. 1 (2017): 32-39.
- [12] Celebi, Hande, and Elif Gunes. "Combined effect of a plasticizer and carvacrol and thymol on the mechanical, thermal, morphological properties of poly (lactic acid)." *Journal of Applied Polymer Science* 135, no. 8 (2018): 45895.
<https://doi.org/10.1002/app.45895>
- [13] Zorah, Mohammed, Izan Roshawaty Mustapa, Norlinda Daud, J. H. Nahida, and N. A. S. Sudin. "Effects of Tributyl Citrate Plasticizer on Thermomechanical Attributes of Poly Lactic Acid." *Journal of Advanced Research in Fluid Mechanics and Thermal Sciences* 62, no. 2 (2019): 274-284.
- [14] Mallick, Shoaib, Zubair Ahmad, Farid Touati, Jolly Bhadra, R. A. Shakoore, and N. J. Al-Thani. "PLA-TiO₂ nanocomposites: Thermal, morphological, structural, and humidity sensing properties." *Ceramics International* 44, no. 14 (2018): 16507-16513.
<https://doi.org/10.1016/j.ceramint.2018.06.068>
- [15] Rasal, Rahul M., Amol V. Janorkar, and Douglas E. Hirt. "Poly (lactic acid) modifications." *Progress in Polymer Science* 35, no. 3 (2010): 338-356.
<https://doi.org/10.1016/j.progpolymsci.2009.12.003>
- [16] Pantani, Roberto, Giuliana Gorrasi, Giovanni Vigliotta, Marius Murariu, and Philippe Dubois. "PLA-ZnO nanocomposite films: Water vapor barrier properties and specific end-use characteristics." *European Polymer*

- Journal 49, no. 11 (2013): 3471-3482.
<https://doi.org/10.1016/j.eurpolymj.2013.08.005>
- [17] Luo, Yan-Bing, Xiu-Li Wang, Da-Yun Xu, and Yu-Zhong Wang. "Preparation and characterization of poly (lactic acid)-grafted TiO₂ nanoparticles with improved dispersions." *Applied Surface Science* 255, no. 15 (2009): 6795-6801.
<https://doi.org/10.1016/j.apsusc.2009.02.074>
- [18] Weir, Alex, Paul Westerhoff, Lars Fabricius, Kiril Hristovski, and Natalie Von Goetz. "Titanium dioxide nanoparticles in food and personal care products." *Environmental Science & Technology* 46, no. 4 (2012): 2242-2250.
<https://doi.org/10.1021/es204168d>
- [19] Baek, Naerin, Young T. Kim, Joe E. Marcy, Susan E. Duncan, and Sean F. O'Keefe. "Physical properties of nanocomposite polylactic acid films prepared with oleic acid modified titanium dioxide." *Food Packaging and Shelf Life* 17, no. 9 (2018): 30-38.
<https://doi.org/10.1016/j.fpsl.2018.05.004>
- [20] Li, Wenhui, Cheng Zhang, Hai Chi, Lin Li, Tianqing Lan, Peng Han, Haiyan Chen, and Yuyue Qin. "Development of antimicrobial packaging film made from poly (lactic acid) incorporating titanium dioxide and silver nanoparticles." *Molecules* 22, no. 7 (2017): 1170.
<https://doi.org/10.3390/molecules22071170>
- [21] Segura González, Edwin A., Dania Olmos, Miguel Ángel Lorente, Itziar Vélaz, and Javier González-Benito. "Preparation and characterization of polymer composite materials based on PLA/TiO₂ for antibacterial packaging." *Polymers* 10, no. 12 (2018): 1365.
<https://doi.org/10.3390/polym10121365>
- [22] Zhang, Jinfeng, Peng Zhou, Jianjun Liu, and Jiaguo Yu. "New understanding of the difference of photocatalytic activity among anatase, rutile and brookite TiO₂." *Physical Chemistry Chemical Physics* 16, no. 38 (2014): 20382-20386.
<https://doi.org/10.1039/C4CP02201G>
- [23] Ramos, Marina, Elena Fortunati, Mercedes Peltzer, Alfonso Jimenez, José María Kenny, and María Carmen Garrigós. "Characterization and disintegrability under composting conditions of PLA-based nanocomposite films with thymol and silver nanoparticles." *Polymer Degradation and Stability* 132, no. 11 (2016): 2-10.
<https://doi.org/10.1016/j.polymdegradstab.2016.05.015>
- [24] Lim, L-T., Rafael Auras, and Maria Rubino. "Processing technologies for poly (lactic acid)." *Progress in Polymer Science* 33, no. 8 (2008): 820-852.
<https://doi.org/10.1016/j.progpolymsci.2008.05.004>
- [25] Valapa, Ravi Babu, G. Pugazhenth, and Vimal Katiyar. "Effect of graphene content on the properties of poly (lactic acid) nanocomposites." *Rsc Advances* 5, no. 36 (2015): 28410-28423.
<https://doi.org/10.1039/C4RA15669B>
- [26] Nunes, Silvana Manske, Marcelo Estrella Josende, Michael González-Durruthy, Caroline Pires Ruas, Marcos Alexandre Gelesky, Luis Alberto Romano, Daniele Fattorini, Francesco Regoli, José Maria Monserrat, and Juliane Ventura-Lima. "Different crystalline forms of titanium dioxide nanomaterial (rutile and anatase) can influence the toxicity of copper in golden mussel *Limnoperna fortunei*?" *Aquatic Toxicology* 205 (2018): 182-192.
<https://doi.org/10.1016/j.aquatox.2018.10.009>
- [27] Haque, Fozia Z., Ruchi Nandanwar, and Purnima Singh. "Evaluating photodegradation properties of anatase and rutile TiO₂ nanoparticles for organic compounds." *Optik* 128 (2017): 191-200.
<https://doi.org/10.1016/j.jilleo.2016.10.025>
- [28] Frone, Adriana Nicoleta, Denis Mihaela Panaitescu, Ioana Chiulan, Augusta Raluca Gabor, Cristian Andi Nicolae, Madalina Oprea, Marius Ghiurea, Dan Gavrilescu, and Adrian Catalin Puitel. "Thermal and mechanical behavior of biodegradable polyester films containing cellulose nanofibers." *Journal of Thermal Analysis and Calorimetry* 138, no. 4 (2019): 2387-2398.
<https://doi.org/10.1007/s10973-019-08218-4>
- [29] Zhou, Yinghui, Liang Lei, Bo Yang, Jianbo Li, and Jie Ren. "Preparation and characterization of polylactic acid (PLA) carbon nanotube nanocomposites." *Polymer Testing* 68 (2018): 34-38.
<https://doi.org/10.1016/j.polymertesting.2018.03.044>
- [30] Mustapa, Izan R., Robert A. Shanks, and Norlinda Daud. "Morphological structure and thermomechanical properties of hemp fibre reinforced poly (lactic acid) Nanocomposites plasticized with tributyl citrate." *Materials Today: Proceedings* 5, no. 1 (2018): 3211-3218.
<https://doi.org/10.1016/j.matpr.2018.01.130>
- [31] Wang, Wei-Wei, Chang-Zhen Man, Chun-Mei Zhang, Long Jiang, Yi Dan, and Thien-Phap Nguyen. "Stability of poly (L-lactide)/TiO₂ nanocomposite thin films under UV irradiation at 254 nm." *Polymer Degradation and Stability* 98, no. 4 (2013): 885-893.

-
- <https://doi.org/10.1016/j.polymdegradstab.2013.01.003>
- [32] Luo, Yan-Bing, Wen-Da Li, Xiu-Li Wang, Da-Yun Xu, and Yu-Zhong Wang. "Preparation and properties of nanocomposites based on poly (lactic acid) and functionalized TiO₂." *Acta Materialia* 57, no. 11 (2009): 3182-3191.
<https://doi.org/10.1016/j.actamat.2009.03.022>
- [33] Costa, Rodrigo GF, Glaucia S. Brichi, Caue Ribeiro, and Luiz HC Mattoso. "Nanocomposite fibers of poly (lactic acid)/titanium dioxide prepared by solution blow spinning." *Polymer Bulletin* 73, no. 11 (2016): 2973-2985.
<https://doi.org/10.1007/s00289-016-1635-1>